IBRACON

IBRACON Structures and Materials Journal

Revista IBRACON de Estruturas e Materiais

ISSN 1983-4195 ismj.org

SciELO

ORIGINAL ARTICLE

Cross-correlation for feature extraction applied to ultrasonic test for stress evaluation in concrete

Correlação-cruzada para extração de características aplicada a ensaio ultrassônico para avaliação de tensão em concreto

Rafaella Moreira Lima Gondim[a]
Karen Fernanda Bompan[a]
Vladimir Guilherme Haach[a]

[a]Universidade de São Paulo – USP, Escola de Engenharia de São Carlos, Departamento de Engenharia de Estruturas, São Carlos, SP, Brasil

Received 11 March 2022
Accepted 29 August 2022

Abstract: Changes in the stress state of a solid medium cause small variations in wave propagation velocities. Cross-correlation (CC) is a tool used for similarity evaluations between two data series. This paper addresses the use of the CC function for the feature extraction of ultrasonic test data that evaluated the stress state in a concrete specimen subjected to compressive loads. The CC function was applied to waveforms, and an analysis of influential parameters (e.g., CC-Domain, time window, and center-time) assessed the differences between the various stress levels. The results showed the variations in $\Delta V/V_0$ vs. stress diagrams were lower in the elastic regime, whereas the analyzed parameters highly influenced the results. S-waves were more suitable for analyses of stress variation, since they were little influenced by time window and center-time.

Keywords: non-destructive tests; ultrasound; acoustoelasticity; direct waves; anisotropy.

Resumo: Mudanças no estado de tensões de um meio sólido causam pequenas variações nas velocidades de propagação de ondas mecânicas. A Correlação Cruzada (CC) é uma ferramenta utilizada para avaliação de similaridade entre dois conjuntos de dados. Este artigo aborda o uso da função CC para extração de características em dados de ensaios ultrassônicos que avaliam o estado de tensões em um corpo de prova de concreto submetido a carregamentos de compressão. A função CC foi aplicada aos sinais, e uma análise dos parâmetros relevantes (e.g., Domínio-CC, janela de tempo e tempo central) avaliou as diferenças entre os vários níveis de tensão. Os resultados mostraram que as variações nos diagramas $\Delta V/V_0$ *vs.* tensão foram menores no regime elástico, enquanto os parâmetros analisados tiveram grande influência sobre o resultado. Ondas secundárias foram mais adequadas para análises de variação de tensão por serem menos influenciadas por tamanho da janela e tempo central.

Palavras-chave: ensaios não destrutivos; ultrassom; acustoelasticidade; ondas diretas; anisotropia.

How to cite: R. M. L. Gondim, K. F. Bompan, and V. G. Haach, "Cross-correlation for feature extraction applied to ultrasonic test for stress evaluation in concrete," *Rev. IBRACON Estrut. Mater.*, vol. 16, no. 4, e16402, 2023, https://doi.org/10.1590/S1983-41952023000400002.

1 INTRODUCTION

The emission of mechanical waves of above 20 kHz frequencies in a structural element is a nondestructive test, called ultrasonic pulse velocity (UPV) [1], usually applied for investigations of damages and material homogeneity and obtaining of mechanical properties [2]-[7]. Hughes and Kelly [8] demonstrated the stress state in a solid medium

Corresponding author: Rafaella Moreira Lima Gondim. E-mail: rresende@usp.br

Financial support: The funding for this research was provided by FAPESP – Fundação de Amparo à Pesquisa do Estado de São Paulo (grants nº 2016/24446-6 and 2017/24096-8) and Coordenação de Aperfeiçoamento de Pessoal de Nível Superior – Brasil (CAPES) - Finance Code 001. The second author was supported by CNPq (Brazilian government agency for research – Nº 302479/2017-1).

Conflict of interest: Nothing to declare.

Data Availability: The data that support the findings of this study are available from the corresponding author, R. M. L. G., upon reasonable request.

influences the propagation velocity of mechanical waves. The phenomenon, called acoustoelastic effect, has been explored for evaluations of the stress state in several materials [9]-[11]. Lillamand et al. [12] verified this effect in concrete, analyzing the influence of stress level on the velocity of compression and transversal waves propagated in cylindric samples subjected to different compression loads. Authors concluded that longitudinal and transversal waves polarized along the direction of loading are more sensitive to the acoustoelastic effect, but the scattering caused by the material hindered ultrasonic velocity measurements [12]. Shokouhi et al. [13] evaluated the combination of damage and acoustoleastic effects in concrete prisms through compression tests with specimens and emission of ultrasonic waves during loading and unloading procedures and detected lower wave velocities in the unloading phase for a same stress level resulting from the mechanical damage caused to the concrete during loading. Bompan and Haach [14] performed ultrasonic tests in concrete prisms subjected to uniaxial compression and observed pre-loadings changed the acoustoelastic behavior due to the Kaiser effect related to the crack generated in concrete elements by the loading.

The propagation velocity of mechanical waves in a solid medium is not influenced by the stress state only in the elastic regime of the material behavior. Several researchers have extended the concepts of acoustoelasticity theory for evaluations of solids with plastic deformation and have called this interaction acoustoplasticity [15]-[17]. Belchenko et al. [18] studied the applicability of the acoustoelasticity method for the estimation of the strain-stress state of dilute aluminum manganese alloy specimens under cyclic loading in the presence of elastic and plastic strains and observed a dependence of stress state on the velocity measurements from the early stages of loading until the fracture of the sample. Mohammadi and Fesharaki [19] investigated the ability of the ultrasonic test to measure stress in both elastic and plastic limits in metal specimens using critically refracted longitudinal (LCR) waves and introducing acoustoplastic constants. LCR are bulk longitudinal waves that propagate parallel to the surface of the specimen.

Changes in the stress state of a solid lead to very small variations in the values of the propagated velocities, which requires an accurate feature extraction methodology. The simplest strategy involves an evaluation of the time-of-flight (TOF) of ultrasonic waves in unperturbed and perturbed media and calculation of the relative velocity variation with the use of path length. However, it may lead to some imprecise results due to difficulties in the definition of the exact time of arrival of compression and transversal waves.

Cross-correlation is a powerful tool widely used in several research areas (e.g., engineering, economics, statistics, medicine, etc.) for comparisons between two series. The cross-correlation function provides a measure of similarity between two signals (perturbed and unperturbed) through the translation of the first signal in the time axis. The coda wave interferometry (CWI), commonly used for evaluations of the acoustoelastic effect, is an example of the application of the CC function. CWI is based on a cross-correlation of two wave signals emitted in unperturbed (no stress) and perturbed (a stress state) media in the tail of the waveform [20]-[24]. Coda waves correspond to scattered waves of late arrival and longer travel-times [20]. According to Planès and Larose [25], the main advantage of the use of these waves is their very high sensitivity to weak perturbations in a medium. Two variations of the method, called doublet and stretching methods, are based on measurements of the time shift and stretching of the time axis of the perturbed signal, respectively [25], [26].

According to the doublet method, a $2T$ time window is moved in the time axis by a time shift t_s around a center-time t_c of the perturbed signal. The cross-correlation function (CC) is calculated for each t_s. The value of time shift that maximizes CC, t_{sMaxCC}, corresponds to the time delay between unperturbed and perturbed signals. This procedure can be adopted for different values of t_c, therefore, the method evaluates the time shifts in consecutive time windows at different t_c. The normalized cross correlation function is applied according to Equation 1, where u_{unp} and u_{per} are unperturbed and perturbed signals, respectively [25], [27], [28], and its value ranges from -1 to 1, periodically, if the time shift is the only difference of the series.

$$CC(t_s) = \frac{\int_{t_c-T}^{t_c+T} u_{unp}(t) u_{pert}(t-t_s) dt}{\sqrt{\int_{t_c-T}^{t_c+T} u_{unp}^2(t) dt \int_{t_c-T}^{t_c+T} u_{pert}^2(t) dt}} \tag{1}$$

Grêt et al. [28] reported the relative velocity variation ($\Delta V/V_0$) can be obtained by Equation 2, where V_0 is the wave velocity in the unperturbed medium.

$$\frac{\Delta V}{V_0} = -\frac{t_{sMaxCC}}{t_c} \tag{2}$$

On the other hand, in the stretching method, the perturbed signal, u_{pert}, is stretched or compressed from $u_{pert}(t)$ to $u_{pert}[t(1+\tau)]$ according to a factor τ for simulating the velocity variation from V to $V(1+\tau)$. The similarity between unperturbed and perturbed signals, u_{unp} and u_{pert}, respectively, is evaluated by normalized cross correlation function $CC(\tau)$ within a $2T$ time window, as showed in Equation 3. The value of τ that maximizes CC (τ_{MaxCC}) is the relative velocity variation, $\Delta V/V_0$, corresponding to the analysis conducted with the window central time, t_c.

$$CC(\tau) = \frac{\int_{t_c-T}^{t_c+T} u_{unp}(t)u_{pert}(t(1+\tau))dt}{\sqrt{\int_{t_c-T}^{t_c+T} u_{unp}^2(t)dt \int_{t_c-T}^{t_c+T} u_{pert}^2(t)dt}} \tag{3}$$

Hadziioannou et al. [29] compared the use of doublet and stretching methods to verify small velocity changes in a medium with an agar-agar gel solution. The authors observed that, although demanding more computational costs, the stretching technique was more stable with respect to noise in the data. Authors also showed that cross-correlation techniques are valid to determine velocity variation even with low signal-to-noise ratios if there is a stable source signal.

Cross-correlation methods applied to time series are dependent on some variables, e.g., time window length, center-time of the window, and range of time shift. Payan et al. [30] employed the CWI doublet method and acoustoelasticity to obtain the coefficients defined by Murnaghan [31] in concrete samples. They applied a loading so as not to exceed 30% of the ultimate strength and remain in the elastic regime. The CWI analysis was performed with a center-time variation, and the results indicated a constant relative velocity variation for compressional waves. Niederleithinger et al. [32] compared relative velocity variation *vs.* stress obtained by TOF and CWI procedures and concluded CWI displays greater sensitivity to stress and damage in concrete cubes. However, they highlighted CWI and TOF results are not immediately comparable, since TOF is related to direct waves, whereas CWI evaluates a weighted average of different wave type velocities. As the authors used CWI, the cross-correlation procedure was only applied to waves of late arrival.

Although CWI is largely used in research on acoustoelastic and damage effects through ultrasonic tests, the literature lacks information on the application of cross-correlation methods for feature extraction in earlier parts of the signal, close to the arrival of longitudinal and transversal waves. Additionally, determination of parameters used for cross-correlation outside the elastic regime requires further investigation. Therefore, this paper discusses the parameters of cross correlation for feature extraction applied to longitudinal and transversal waves from ultrasonic tests to evaluate the stress state in concrete.

2 METHODOLOGY AND EXPERIMENTAL PROGRAM

This section describes the proposed methodology for the assessment of cross-correlation as a method for feature extraction applied to ultrasonic tests for stress evaluation in concrete. The main steps of this work are shown in Figure 1. Description of material properties and test specimens are found in Section 2.1 and Section 2.2, respectively. After characterization tests, ultrasonic tests were conducted in a prismatic specimen to evaluate the influence of stress level on the ultrasonic pulse velocity (UPV), as described in Section 2.3. The cross-correlation procedure was applied to the recorded ultrasonic waveforms and an analysis of the influential parameters assessed the differences between the applications of low and high stresses, as detailed in Section 2.4.

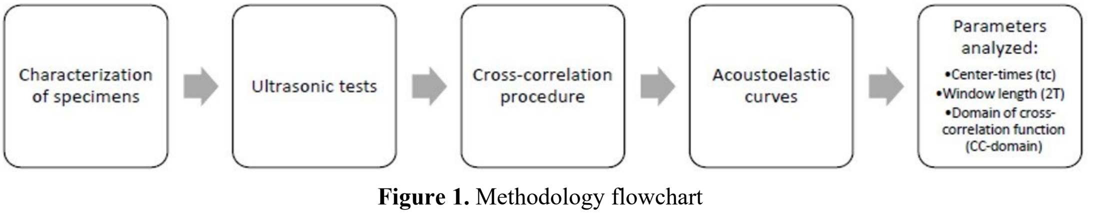

Figure 1. Methodology flowchart

2.1 Material properties

The materials applied to this research were chosen aiming to obtain a conventional concrete. The concrete mix used was composed of Type III Portland cement of high early strength, as specified by ASTM [33], sand of 2.36 mm maximum size and 2.00 fineness modulus, and gravel of 19 mm maximum size and 6.73 fineness modulus. Both maximum size and fineness modulus of the aggregates were in accordance with ABNT [34], and the proportions of materials in mass for the production of the concrete were 1:1.30:2.20 (cement:sand:gravel). The water/cement ratio was 0.43 and the material had a 150 mm slump. The concrete composition reached a 30.62 MPa average compressive strength at 28 days, with a 13.45% coefficient of variation.

2.2 Test specimens

Four 150 mm x 150 mm x 500 mm prismatic specimens were molded and kept in laboratory for 24 h after casting. The molds were then removed, and the specimens were kept in a moist chamber for curing. At day 28, three prisms were tested under compression towards the definition of the average compressive strength (f_{cm}) of the samples. Ultrasonic tests were performed with the remaining sample at ages higher than 28 days.

2.3 Ultrasonic tests

Two 250 kHz transducers of 2.00 µs pulse width arranged in a through-transmission setting were used in the ultrasonic tests, and longitudinal and transversal waves were propagated to the tested specimens. A couplant paste specific for the transmission of normal incidence transversal waves was used in the sample-transducer interface. Pundit Lab+ and Pundit Link by Proceq® were, respectively, the ultrasound equipment and the software that obtained the ultrasound signals. The experimental values were recorded every 0.5 µs since the acquisition frequency of the equipment was 2 MHz. The UPV variation was analyzed in two directions, i.e., parallel and perpendicular to the loading direction, called axes 1 and 2, respectively (Figure 2a). The total recording times used in the ultrasonic tests were 360 µs (direction 1) and 120 µs (direction 2).

The ultrasonic tests were performed in a sample subjected to uniaxial compression (see Figure 2a for the experimental setup). A steel frame fixed to a reaction slab and equipped with a hydraulic jack applied the load. Two U-shaped steel plates were positioned above and under the sample (Figure 2b) for safely placing the transducers in an area not subjected to loading for the avoidance of damage to the equipment. Polystyrene pieces (Figure 2c) kept the transducers in contact with the prism surface when the waves were emitted in the direction of the loading, and in place by a rubber strip when the waves were emitted transversally to the loading direction. The transducers were positioned in the center of the corresponding surface of the sample, as shown in Figure 2c and Figure 2d.

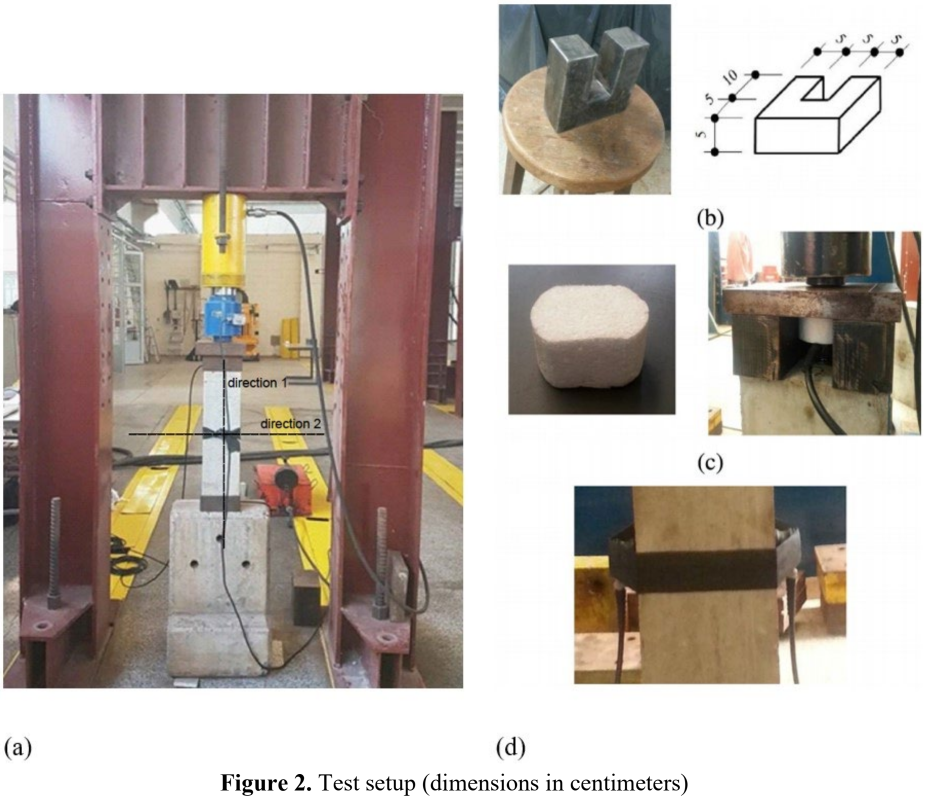

Figure 2. Test setup (dimensions in centimeters)

The longitudinal waves were called LW_{ij}, and the transversal waves were denoted by TW_{ij}, where i represents the axis of propagation of the wave and j is the polarization direction.

Twelve loading cycles were applied to the specimen. A maximum stress ($\sigma_{Max,UPV}$) was applied in each cycle, corresponding to approximately 60% of the compressive strength (f_{cm}) equivalent to a force of 440 kN. Bompan and Haach [14] demonstrated UPV variation due to the acoustoelastic effect shows high variability over the first loading cycles. However, there is a trend to a stable behavior as more loading cycles are applied. Towards avoiding this initial variation, the first ten cycles consisted only of pre-loading prior to the ultrasonic tests - no UPV measurements were recorded. The ultrasound test was performed in the unloading phases of the 11^{th} and 12^{th} cycles and the measurements were taken for every 20 kN decrement (22 decrements). According to Shokouhi et al. [13], new cracks are opened only when the applied load exceeds the maximum load of the previous step. Although some cracks propagate due to creep even if the applied load has not exceeded the maximum history load, the influence of new damage will be reduced in the results of the UPV tests performed during unloading. LW_{11} and TW_{12} were emitted in the 11^{th} unloading phase, and LW_{22} and TW_{21} were analyzed in the 12^{th} unloading cycle. The ultrasound signal for each load value was established by the average of ten pulses. The experimental program flowchart is shown on Figure 3.

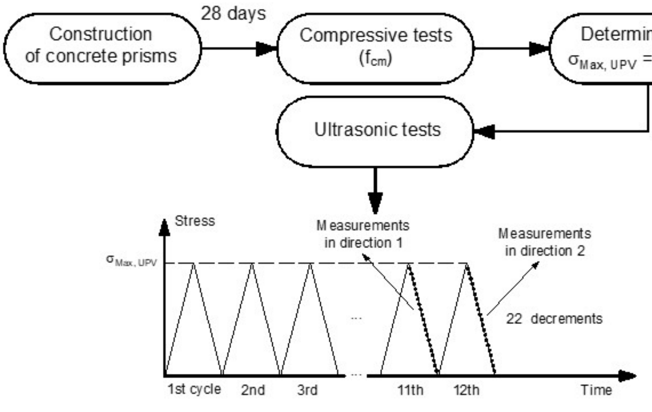

Figure 3. Experimental program flowchart

2.4 Procedures of feature extraction

Figure 4 shows the waveforms used as references in the UPV analyses. Longitudinal waves were the first to arrive, followed by transversal ones, indicated by an increase in the amplitudes. Arrival of these waves are indicated by grey circles in Figure 4. Cross-correlation was performed according to Equation 1 and the relative velocity variation was obtained by Equation 2.

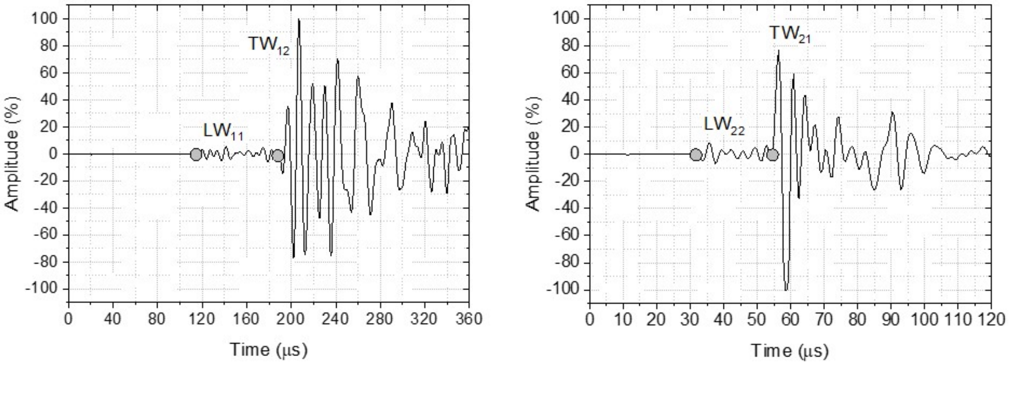

(a) (b)

Figure 4. Reference waveforms obtained in UPV experiments: (a) direction 1 and (b) direction 2

The cross-correlation function was applied to parts of the waveform. These parts, named as time windows, are identified by a center-time, t_c, representing the middle time of the extracted time window; and by a window length, $2T$, that represents the size of the window defined between the points [t_c - T, t_c + T], see Figure 5. In addition, the cross-correlation function was applied to a range of time-shift values (t_s) defining the CC-domain.

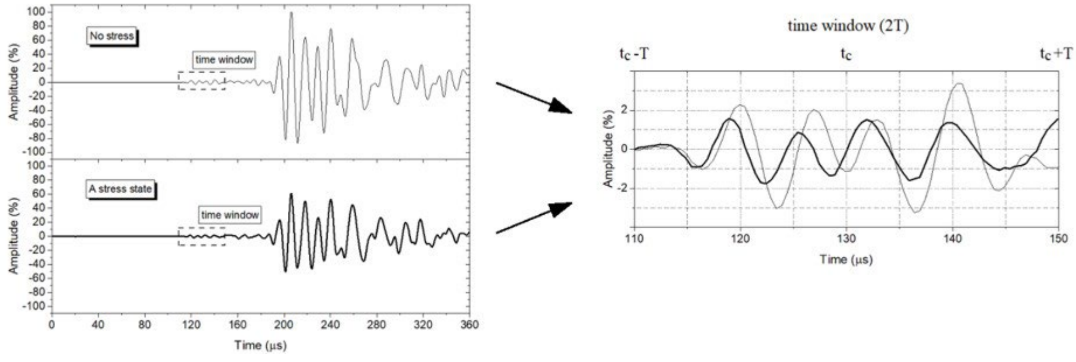

Figure 5. Typical time window variables in the feature extraction procedure.

Finally, the feature extraction analysis was performed following the sequence:

a) Construction of $\Delta V/V_0$ *vs.* σ curves using direct waves,
b) Evaluation of the CC-Domain variation in the generation of the $\Delta V/V_0$ *vs.* σ curves,
c) Evaluation of the t_c variation in the generation of the $\Delta V/V_0$ *vs.* σ curves,
d) Evaluation of the 2T variation in the generation of the $\Delta V/V_0$ *vs.* σ curves,

The range of values of t_c and 2T used in the analyzes could not be standardized for all ultrasonic waves because they were chosen according to the respective waveform.

3 EXPERIMENTAL RESULTS

The experimental results show the evaluation of the relative velocity variation as a function of compressive stress for the studied prism. In case of prism with no stress, velocity values LW_{11}, LW_{22}, TW_{12}, and TW_{21} were 4332 m/s, 4733 m/s, 2624 m/s, and 2736 m/s, respectively. All diagrams in Figure 6 show the effect of stress level on the relative velocity variation. According to Mehta and Monteiro [35], below approximately 30% of the compressive strength, the interfacial transition zone cracks remain stable; therefore, the stress *vs.* strain curve remains linear. This limit is commonly admitted for the elastic behavior of concrete - here, the value was 10.20 MPa. The dependence of UPV on the stress level may also be observed for stress levels over the elastic limit.

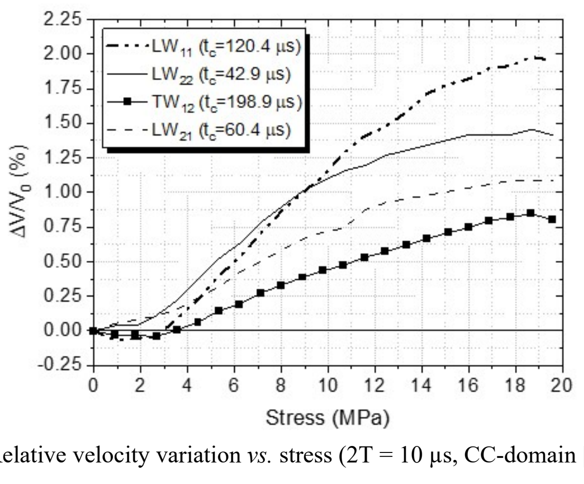

Figure 6. Relative velocity variation *vs.* stress (2T = 10 µs, CC-domain [-4 µs, 4 µs])

The diagrams in Figure 6 were obtained from specific center-times, window length, and *CC-domain*. Figure 7 displays the relative velocity variation *vs.* stress for longitudinal waves LW_{11} with the same values of center-time and window length displayed in Figure 6, equal to 120.4 µs and 10 µs, respectively, but with different *CC-domain*. The change in the *CC-domain* in the analysis generated an abrupt increase in the relative velocity variation.

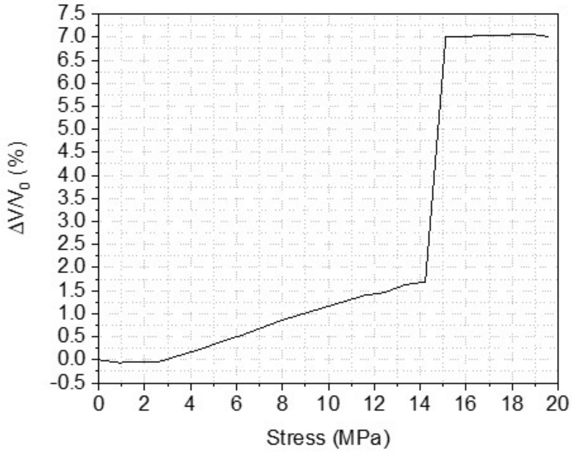

Figure 7. Relative velocity variation *vs.* stress for LW_{11} (t_c = 120.4 µs; 2T = 10 µs; CC-domain [-10 µs, 10 µs])

This sudden increase in $\Delta V/V_0$ values occurs because the cross-correlation function has several local maximums in domain [-10 µs, 10 µs], see Figure 8. For low stress levels, the argument of the global maximum in domain [-10 µs, 10 µs] is approximately 1 µs, which gradually increases with the stress level increase. However, once the stress reaches 13.3 MPa (≈ 43% of compressive strength), the argument of the global maximum value of *CC* in this domain abruptly changes to a value around 7 µs, causing the curve discontinuity showed in Figure 7. A smaller domain for the *CC* function provided the diagram in Figure 6, suggesting the analysis of the variation in UPV with stress level should evaluate the behavior of the same local maximum peak of the *CC* function as it changes with the stress increase.

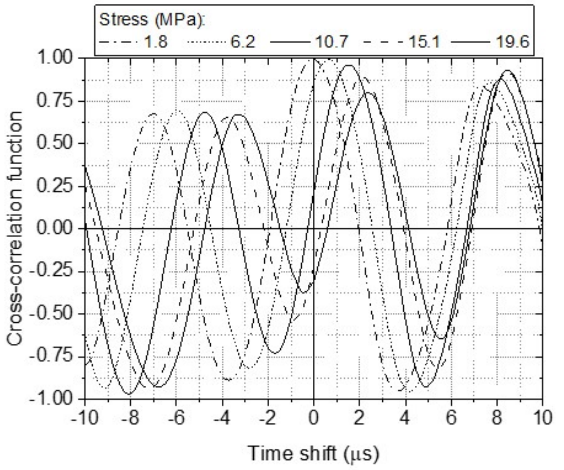

Figure 8. Cross-correlation function for LW_{11} (t_c = 120.4 µs; 2T = 10 µs)

Figure 9 displays the maximum value of the cross-correlation function and relative velocity variation for longitudinal and transversal waves, LW_{11} and TW_{12}, respectively, considering different center-times t_c. Both waves were influenced by the center-time in the evaluated ranges; however, longitudinal waves showed the highest variations.

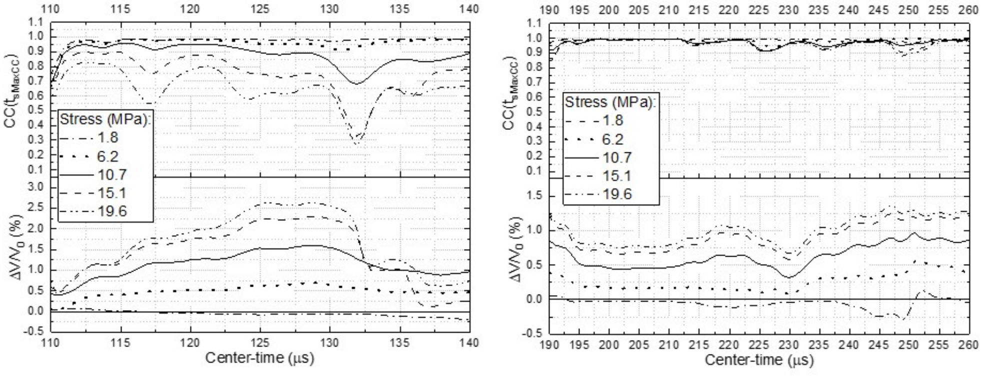

(a) (b)

Figure 9. Maximum value of the Cross-correlation function and relative velocity variation *vs.* center-time (2T = 10 μs; CC-domain [-1 μs, 4 μs]): (a) LW_{11} and (b) TW_{12}

The mean values of the relative velocity variation for LW_{11} in the 110 μs and 140 μs range were 0.49% with a 30.97% coefficient of variation for 6.2 MPa stress, and 1.4% with a 50.82% coefficient of variation for 15.1 MPa stress. TW_{12} were less influenced by the center-time variation. The mean value of the relative velocity variation in the 190 μs and 260 μs range for 6.2 MPa stress was 0.53% with 20.59% coefficient of variation. Differently from longitudinal waves, TW_{12} showed small variations with the center-time even for high stress. The relative velocity variation was 0.89% with a 14.82% coefficient of variation for 15.1 MPa stress. A decrease in the maximum value of the cross-correlation function was observed as the compressive stress was applied. *CC* function is a measure of similarity between time series, and a decrease in its value denotes changes in waveforms with the stress application. Such changes are caused by the internal micro-cracking of the material, which produces a scatter of the ultrasonic waves.

Figure 10 shows the relative velocity variation *vs.* stress for longitudinal and transversal waves, LW_{11} and TW_{12}, respectively, considering different center-times t_c. The center-time influence on the curves was smaller in the elastic behavior range; after this limit, the difference between the lowest and the highest $\Delta V/V_0$ for the same stress gradually increased, reaching very high values for LW_{11}.

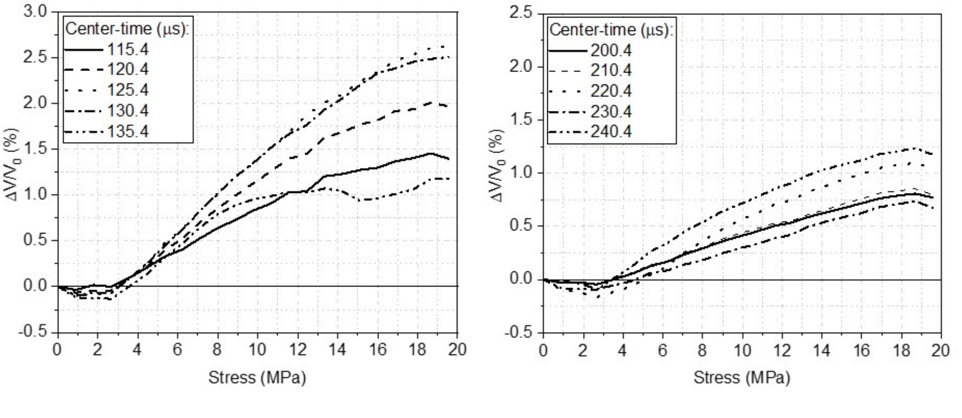

(a) (b)

Figure 10. Relative velocity variation *vs.* stress (2T = 10 μs; CC-domain [-1 μs, 4 μs]): (a) LW_{11} and (b) TW_{12}

In case of longitudinal waves LW_{11}, the relative velocity variation was not calculated for center-times higher than 140 μs because the same local maximum of the *CC* function was not observed in all stress levels, see Figure 11. The

CC local maximum clearly identified for low stresses could not be located for stresses higher than 8.0 MPa. Besides, the cross-correlation function values were very low in domain [-1 µs, 4 µs], indicating a weak similarity between the waveforms in this center-time range.

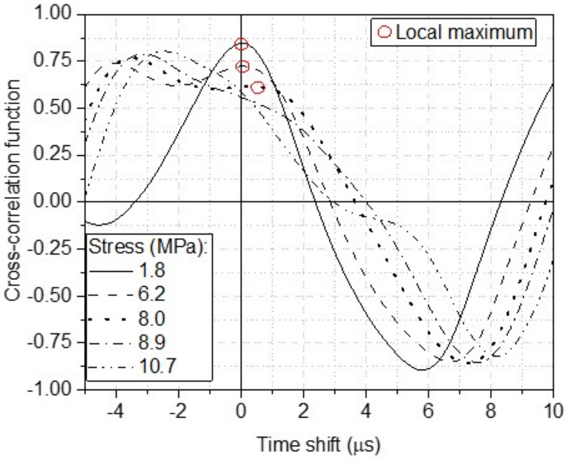

Figure 11. Cross-correlation function for LW_{11} (t_c = 154.4 µs, 2T = 10 µs)

Regarding transversal waves, TW_{12}, the relative velocity variation dependence on the stress continued to be verified for very high center-times such as 350.4 µs, and the analysis characterized Coda Wave Interferometry. However, the relative velocity variation values in such center-times were very different from those in center-times around 194.9 µs (see Figure 12).

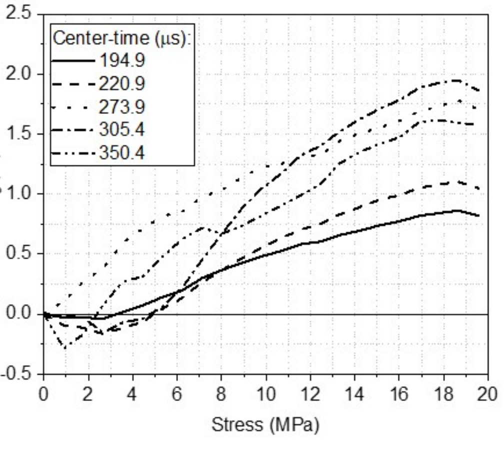

Figure 12. Relative velocity variation *vs.* stress for TW_{12} (2T = 10 µs; CC-domain [-1 µs, 10 µs])

The center-time similarly influenced the results for ultrasonic waves propagated in direction 2 of the prism (Figure 13). However, a high variation in the $\Delta V/V_0$ *vs.* stress curve was observed for different center-times even in the elastic region for longitudinal waves LW_{22} (Figure 14a). On the other hand, transversal waves TW_{21} (Figure 14b) showed very small variations with 55.9 µs to 75.9 µs center-times.

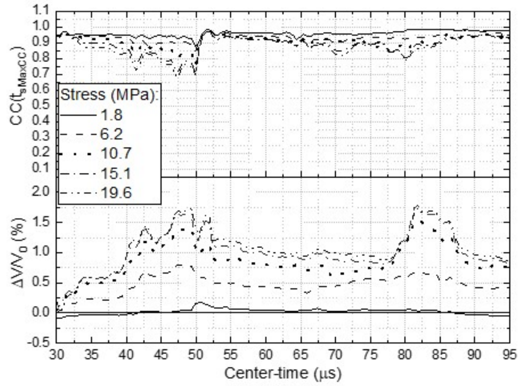

Figure 13. Maximum value of the Cross-correlation function and relative velocity variation *vs.* center-time for waves in the direction 2 (2T = 10 μs; CC-domain [-1 μs, 2 μs])

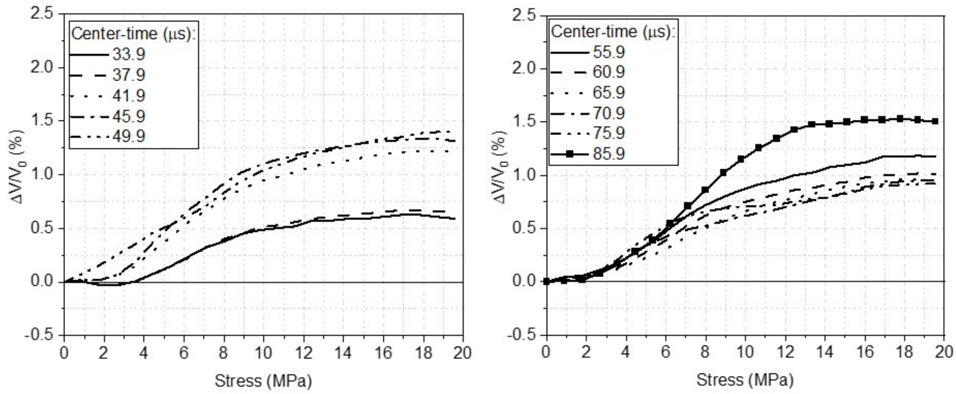

(a) (b)

Figure 14. Relative velocity variation *vs.* stress (2T = 10 μs; CC-domain [-1 μs, 2 μs]): (a) LW_{22} and (b) TW_{21}

Time window (*2T*) also influenced the results obtained from the cross-correlation function. Figures 15, 16 and 17 show high time-windows led to a decrease in the $\Delta V/V_0$ variation through different center-times.

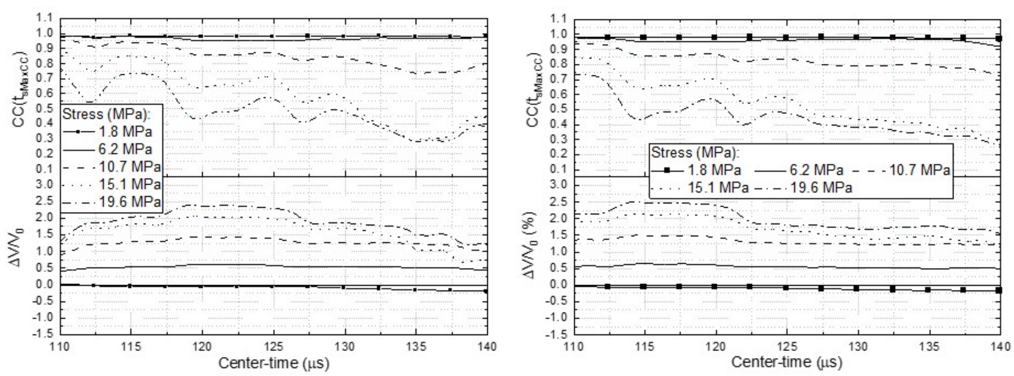

(a) (b)

Figure 15. Maximum value of the Cross-correlation function and relative velocity variation *vs.* center-time for LW_{11} (CC-domain [-1 μs, 4 μs]): (a) 2T = 20 μs and (b) 2T = 30 μs

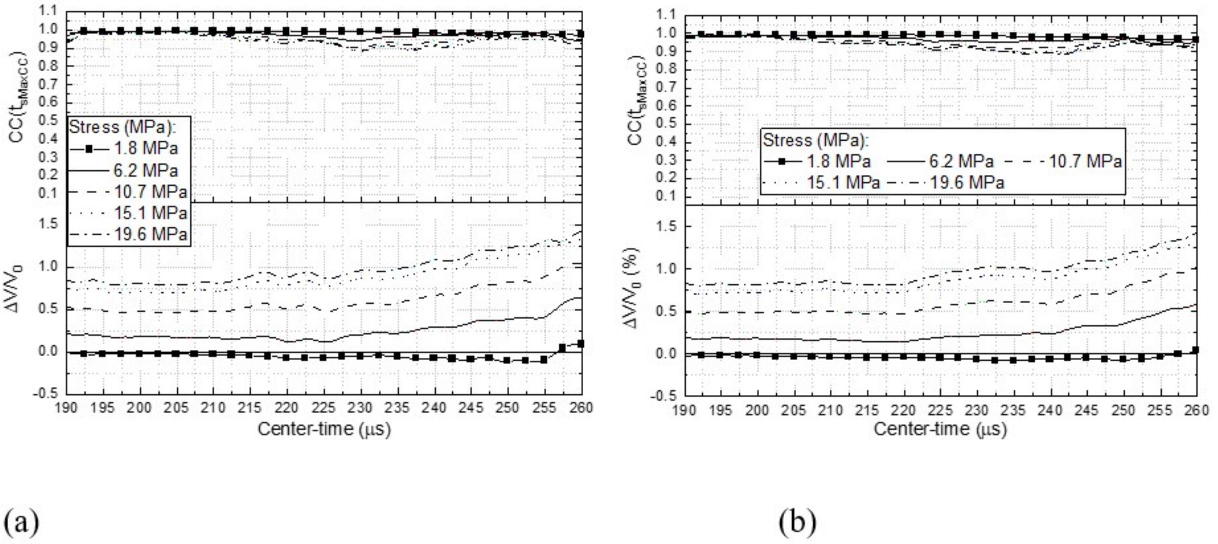

Figure 16. Maximum value of the Cross-correlation function and relative velocity variation *vs.* center-time for TW_{12} (CC-domain [-1 µs, 4 µs]): (a) 2T = 20 µs and (b) 2T = 30 µs

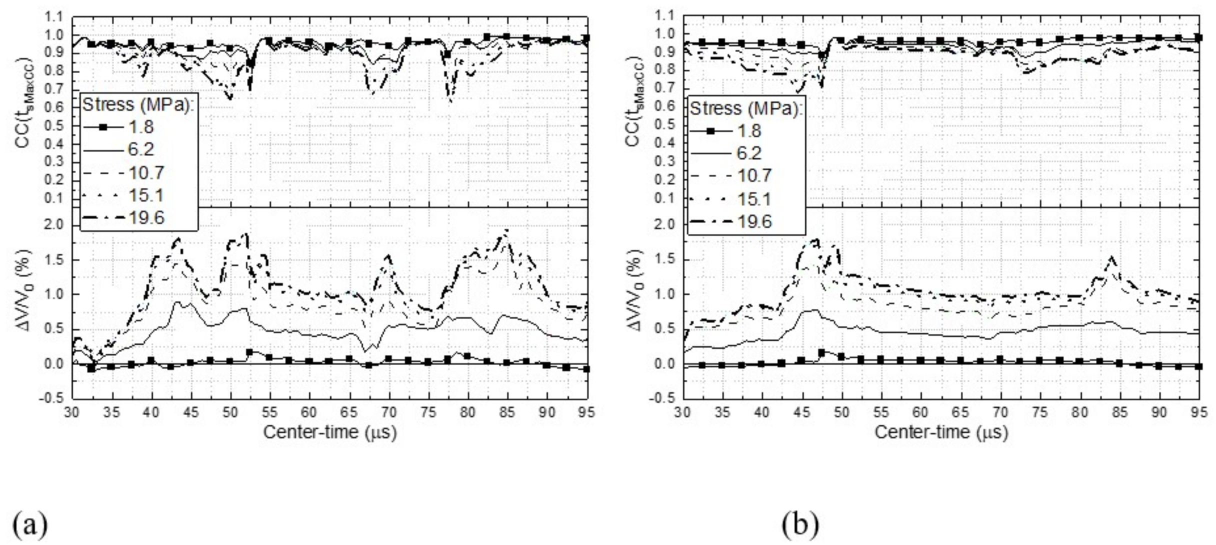

Figure 17. Maximum value of the Cross-correlation function and relative velocity variation *vs.* center-time for waves in the direction 2 (CC-domain [-1 µs, 2 µs]): (a) 2T = 5 µs and (b) 2T = 15 µs

The maximum value of the cross-correlation function was also reduced, indicating a lower similarity ratio between the waveforms inside that time window. This was expected, since a higher amount of data is evaluated due to the time window increase, becoming a more sensitive result to differences between the waveforms.

Figure 18 shows the relative velocity variation *vs.* stress for longitudinal and transversal waves for different time windows. Longitudinal waves were more influenced by the variation in time window in comparison to transversal waves. Regarding $LW_{11,}$ expressive differences were observed for stresses higher than the nominal elastic limit, whereas high differences were observed for LW_{22} even in the elastic region.

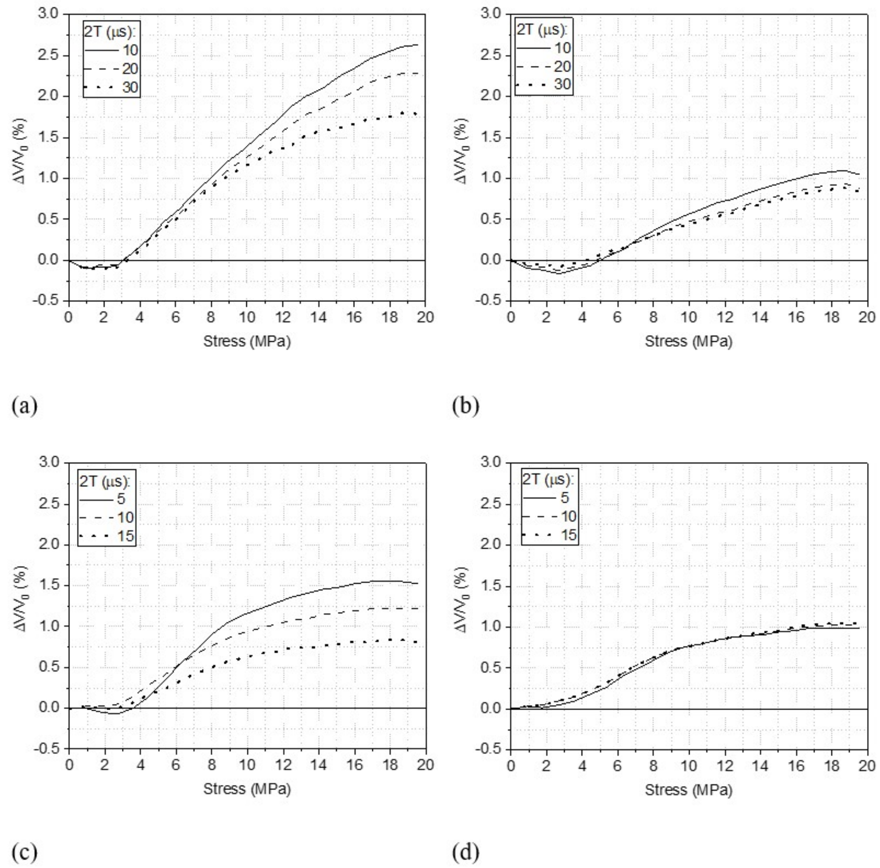

Figure 18. Relative velocity variation *vs.* stress (CC-domain [-1 μs, 4 μs]): (a) LW_{11} (t_c = 125.4 μs), (b) TW_{12} (t_c = 220.4 μs), (c) LW_{22} (t_c = 41.9 μs) and (d) TW_{21} (t_c = 60.4 μs)

4 DISCUSSIONS

The heterogeneity of concrete causes a scatter of the ultrasonic waves, which is increased when a stress level is applied to a concrete element, leading to the creation and extension of microcracks. This effect makes the ultrasonic waves travel along different trajectories inside the specimen from source to receiver. The waveform obtained from the ultrasonic tests in concrete specimens is a composition of the amplitudes of several scattered waves arriving at different times at the receiver. In the cross-correlation for feature extraction, the analysis uses a time window of the waveform, i.e., the relative velocity variation obtained is an average value of all waves arriving in time range. This average represents the exact value of the relative velocity variation in case of an isotropic material, which is constant for all paths. The velocities of compression and transversal waves for an isotropic material are independent of the propagation direction ($V_{11} = V_{22} = V_{33}$ and $V_{12} = V_{23} = V_{13}$). Therefore, in a scenario A where the prism showed in Figure 19 is composed of an isotropic material, velocities V_A , V_B, and V_C related to paths S_A, S_B, and S_C, respectively, are equal, although the TOFs and the paths are different ($t_A \neq t_B \neq t_C$ and $S_A \neq S_B \neq S_C$, respectively). If the material remains isotropic after a stress state, the relative velocity variations ($\Delta V/V_o$) will be the same in all paths.

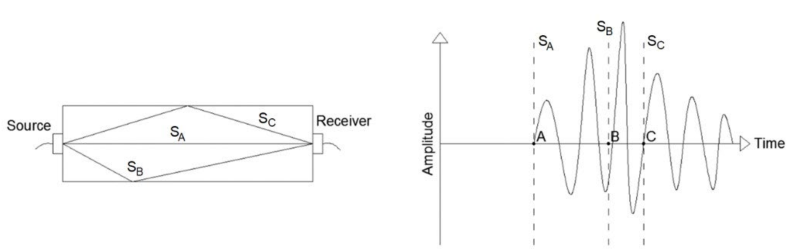

Figure 19. Scheme of wave paths in an ultrasonic waveform

However, Hughes and Kelly [8] showed the stress state changes the constitutive matrix of a material, leading to a dependence of ultrasonic velocity on the stress level. The authors obtained expressions for the stress dependence of the velocities of direct waves using the finite strain formulation of Murnaghan [31], according to which an isotropic material becomes anisotropic due to the stress state. Regarding an anisotropic material, the wave velocities are dependent on the propagation direction ($V_{11} \neq V_{22}$ and $V_{12} \neq V_{21}$). In this scenario, called scenario B, velocities V_A, V_B and V_C (Figure 19) are completely different and dependent on the constitutive matrix of the material. Consequently, the relative velocity variation is not the same for different paths and the $\Delta V/V_o$ value from the cross-correlation function represents an average behavior of multiple waves travelling in distinct paths and arriving at the receiver in the evaluated time window.

The anisotropy level induced by the stress can be expressed as a fractional velocity difference. The more common expression from the literature relates the velocities of transverse ultrasonic waves polarized in mutually perpendicular directions [18], [36]. Here, this concept is extended by other velocities towards the definition of anisotropy dimensionless coefficients α and β for longitudinal and transversal waves, respectively Equation 4 and Equation 5.

$$\alpha = \frac{V_{11}-V_{22}}{(V_{11}+V_{22})/2} \tag{4}$$

$$\beta = \frac{V_{12}-V_{21}}{(V_{12}+V_{21})/2} \tag{5}$$

Concrete displays some level of anisotropy even with no stress application [37]. The anisotropy dimensionless coefficients were 8.85% and 4.18% for longitudinal and transversal waves, respectively, for null stress, showing the anisotropy of the material affects the longitudinal velocity more intensively in the concrete specimen analyzed, and explaining the higher $\Delta V/V_o$ variability with time window or center-time for longitudinal waves in comparison to transversal ones (see section 5).

The anisotropy coefficients were calculated for all stress levels subtracting the coefficients at null stress (α_0 and β_0) to facilitate the comparison between values of longitudinal and transversal waves. The stress application generates a small variation in anisotropy coefficients when compared with the initial values (Figure 20), showing the initial anisotropy of the concrete is the main contributing factor to scenario B, previously described.

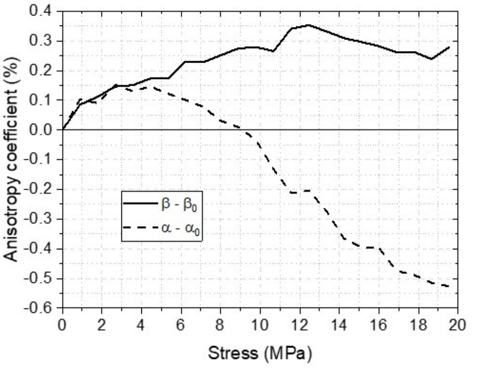

Figure 20. Variation of anisotropy coefficients with the stress level.

Although the $\Delta V/V_o$ value obtained by the cross-correlation function is influenced by the anisotropy of the material and represents the behavior of multiple waves, it remains dependent on the stress level for any center-time or time window, according to the results in section 5; however, it is neither constant with the change in the variables, nor the relative velocity variation of the direct waves - direct waves are those that arrived first at the receiver. Therefore, the time window should be small and the center-time should be closer to the time of arrival of the waves for the $\Delta V/V_o$ obtained by the cross-correlation function to represent direct waves.

5 CONCLUSIONS AND FINAL REMARKS

This study evaluated the influence of cross-correlation function parameters on the feature extraction of ultrasonic test results performed in a concrete prism. The specimen was subjected to different stress levels in/out of the elastic regime, and analyses were conducted for longitudinal and transversal waves emitted in two directions regarding time window length, center-time of the time window, and cross-correlation function domain. The influence of the stress level on the relative velocity variation was observed in all ultrasonic waves in and out the elastic regime. Discussions led to the following conclusions:

- The global maximum value of the *CC* function cannot be used for the calculation of the relative velocity variation in case of high stresses applied to concrete. The *CC* domain should be carefully selected, since the time-shift that represents the relative velocity variation is an argument of a local maximum value.
- Longitudinal waves were more sensitive to changes in time window and center-time than transversal waves, probably due to the anisotropic behavior of the concrete, since the anisotropic dimensionless coefficient for longitudinal waves was higher than that for transversal waves. This behavior made the transversal waves the most suitable for the analysis of stress variation since they are few influenced by the time window and center-time. Therefore, transversal waves, which are lightly influenced by time window and center-time, are the most suitable for analyses of stress variation.
- Variations in $\Delta V/V_0$ *vs.* stress diagrams caused by time window and center-time were lower for stresses in the elastic regime. Although the choice of the time window or center-time highly influences the results from the cross-correlation function, the relative velocity variation remains dependent on the stress level; however, this relation is not representative of direct waves, as the cross-correlation represents the average velocity variation between two time windows.
- The feature extraction procedure applied to the results of ultrasonic tests is a key point in the evaluation of the dependence of the propagation wave velocity on the stress level. The *CC*-function parameters should be carefully selected and kept constant in results that will be compared.

LIST OF ACRONYMS AND SYMBOLS

2T: window length
α: anisotropy dimensionless coefficient for longitudinal waves
β: anisotropy dimensionless coefficient for transversal waves
$\Delta V/V_0$: relative velocity variation
σ: applied compressive stress
$\sigma_{Max,UPV}$: maximum compressive stress applied during UPV tests
τ: factor used to “stretch” or compress the signal in the stretching method
ABNT: Brazilian Association of Technical Standards
ASTM: American Society for Testing and Materials
CC: Cross-Correlation function
CC-domain: domain of cross-correlation function
CWI: Coda Wave Interferometry
f_{cm}: average compressive strength of concrete
LCR: Critically Refracted Longitudinal waves
LW_{ij}: longitudinal waves propagated in direction i and polarized in direction j
S_A, S_B, S_C: possible propagation paths
S-waves: secondary or transversal waves
t_c: center-time
TOF: Time of Flight
t_s: time shift used as argument of the cross-correlation function in the doublet method
t_{sMaxCC}: time shift that generates the maximum value of the cross-correlation function in the doublet method
TW_{ij}: transversal waves propagated in direction i and polarized in direction j
UPV: Ultrasonic Pulse Velocity
u_{pert}: signal recorded in the perturbed medium
u_{unp}: signal recorded in the unperturbed medium
V_0: propagation velocity in the unperturbed medium
V_{ij}: velocity of a wave propagated in direction i and polarized in direction j
V_A, V_B, V_C: velocity of waves traveling through paths S_A, S_B and S_C, respectively

ACKNOWLEDGEMENTS

The authors acknowledge the Laboratory of Structures at the São Carlos Engineering School, where the experimental work was performed, and the funding provided by FAPESP – Fundação de Amparo à Pesquisa do Estado de São Paulo (grants nº 2016/24446-6 and 2017/24096-8) and Coordenação de Aperfeiçoamento de Pessoal de Nível Superior – Brasil (CAPES) - Finance Code 001. The second author was supported by CNPq (Brazilian government agency for research – Nº 302479/2017-1).

REFERENCES

[1] V. M. Malhotra and N. J. Carino, *Handbook on Nondestructive Testing of Concrete*, 2nd ed, Boca Raton, Florida, USA: CRC Press, 2004.

[2] H. Chai, D. Aggelis, S. Momoki, Y. Kobayashi, and T. Shiotani, "Single-side access tomography for evaluating interior defect of concrete," *Constr. Build. Mater.*, vol. 24, no. 12, pp. 2411–2418, 2010, http://dx.doi.org/10.1016/j.conbuildmat.2010.03.003.

[3] F. Benmeddour, G. Villain, O. Abraham, and M. Choinska, "Development of an ultrasonic experimental device to characterise concrete for structural repair," *Constr. Build. Mater.*, vol. 37, pp. 934–942, 2012, http://dx.doi.org/10.1016/j.conbuildmat.2012.09.038.

[4] M. Benaicha, O. Jalbaud, X. Roguiez, A. H. Alaoui, and Y. Burtschell, "Prediction of Self-Compacting Concrete homogeneity by ultrasonic velocity," *Alexandria Eng. J.*, vol. 54, no. 4, pp. 1181–1191, 2015., http://dx.doi.org/10.1016/j.aej.2015.08.002.

[5] V. Haach, L. Juliani, and M. Ravanini, "Ultrasonic evaluation of mechanical properties of concretes produced with high early strength cement," *Constr. Build. Mater.*, vol. 96, pp. 1–10, 2015., http://dx.doi.org/10.1016/j.conbuildmat.2015.07.139.

[6] V. Haach and L. Juliani, "Possibilities of using ultrasound for the technological control of concrete of hollow-core slabs," *Constr. Build. Mater.*, vol. 133, pp. 409–415, 2017, http://dx.doi.org/10.1016/j.conbuildmat.2016.12.121.

[7] S. S. Kumar, J. Krishnamoorthi, B. Ravisankar, and V. Balusamy, "Assessing quality of diffusion bonded joints with interlayer using ultrasonic/ultrasound," *J. Mater. Process. Technol.*, vol. 242, pp. 139–146, 2017., http://dx.doi.org/10.1016/j.jmatprotec.2016.11.036.

[8] D. S. Hughes and J. L. Kelly, "Second-order elastic deformation of solids," *Phys. Rev.*, vol. 92, no. 5, pp. 1145–1149, 1953, http://dx.doi.org/10.1103/PhysRev.92.1145.

[9] C. L. Nogueira, "Ultrasonic evaluation of acoustoelastic parameters in aluminum," *J. Mater, Civ. Eng.*, vol. 29, no. 10, pp. 04017158-1-04017158-9, 2017, http://dx.doi.org/10.1061/(ASCE)MT.1943-5533.0002009.

[10] Q. Zhu, C. Burtin, and C. Binetruy, "The viscoelastic effect during acoustoelastic testing of polyethylene," *Polym. Test.*, vol. 69, pp. 286–292, 2018, http://dx.doi.org/10.1016/j.polymertesting.2018.05.032.

[11] S. Garstev and B. Köhler, "Direct measurements of Rayleigh wave acoustoelastic constants for shot-peened superalloys," *NDT Int.*, vol. 113, pp. 102279, 2020, http://dx.doi.org/10.1016/j.ndteint.2020.102279.

[12] I. Lillamand, J. F. Chaix, M. A. Ploix, and V. Garnier, "Acoustoelastic effect in concrete material under uni-axial compressive loading," *NDT Int.*, vol. 43, no. 8, pp. 655–660, 2010, http://dx.doi.org/10.1016/j.ndteint.2010.07.001.

[13] P. Shokouhi, A. Zoega, and H. Wiggenhauser, "Nondestructive investigation of stress-induced damage in concrete," *Adv. Civ. Eng.*, vol. 2010, pp. 740189, 2010, http://dx.doi.org/10.1155/2010/740189.

[14] K. F. Bompan and V. G. Haach, "Ultrasonic tests in the evaluation of the stress level in concrete prisms based on the acoustoelasticity," *Constr. Build. Mater.*, vol. 162, pp. 740–750, 2018, http://dx.doi.org/10.1016/j.conbuildmat.2017.11.153.

[15] M. Hirao and Y. H. Pao, "Dependence of acoustoelastic birefringence on plastic strains in a beam," *J. Acoust. Soc. Am.*, vol. 77, no. 5, pp. 1659–1664, 1985, http://dx.doi.org/10.1121/1.391964.

[16] Y. H. Pao, "Theory of acoustoelasticity and acoustoplasticity", in *Solid mechanics Research for Quantitative Non-Destructive Evaluation*, J. D. Achenbach, and Y. Rajapakse, Ed., Dordrecht, Netherlands: Martinus Nijhoff Publishers, 1987, ch. 8.1, sec. 8, pp. 257–273.

[17] M. Kobayashi, "Acoustoelastic theory for plastically deformed solids", *JSME Int J.*, vol. 33, no. 3, pp. 310–318, 1990.

[18] V. K. Belchenko, A. M. Lobachev, V. S. Modestov, D. A. Tretyakov and L. V. Shtukin, "An estimation of the strain-stress state under cyclic loading by the acoustoelasticity method", *St. Petersburg Polytechnical Univ. J. Phys. Math.*, vol. 3, no. 1, pp. 71–76, 2017.

[19] M. Mohammadi and J. J. Fesharaki, "Determination of acoustoelastic/acoustoplastic constants to measure stress in elastic/plastic limits by using LCR wave," *NDT Int.*, vol. 104, pp. 69–76, 2019., http://dx.doi.org/10.1016/j.ndteint.2019.04.003.

[20] S. C. Stähler, C. Sens-Schönfelder, and E. Niederleithinger, "Monitoring stress changes in a concrete bridge with coda wave interferometry," *J. Acoust. Soc. Am.*, vol. 129, no. 4, pp. 1945–1952, 2011., http://dx.doi.org/10.1121/1.3553226.

[21] Y. Zhang et al., "Study of stress-induced velocity variation in concrete under direct tensile force and monitoring of the damage level by using thermally-compensated coda wave interferometry," *Ultrasonics*, vol. 52, no. 8, pp. 1038–1045, 2012., http://dx.doi.org/10.1016/j.ultras.2012.08.011.

[22] P. Shokouhi, J. Rivière, C. R. Lake, P. Y. Le Bas, and T. J. Ulrich, "Dynamic acousto-elastic testing of concrete with a coda-wave probe: comparison with standard linear and nonlinear ultrasonic techniques," *Ultrasonics*, vol. 81, pp. 59–65, 2017, http://dx.doi.org/10.1016/j.ultras.2017.05.010.

[23] E. Niederleithinger, X. Wang, M. Herbrand, and M. Muller, "Processing Ultrasonic data by coda wave interferometry to monitor load tests of concrete beams," *Sensors (Basel)*, vol. 18, no. 6, pp. 1971, 2018., http://dx.doi.org/10.3390/s18061971.

[24] H. Zhan, H. Jiang, C. Zhuang, J. Zhang, and R. Jiang, "Estimation of stresses in concrete by using coda wave interferometry to establish an acoustoelastic modulus database," *Sensors (Basel)*, vol. 20, no. 14, pp. 4031, 2020., http://dx.doi.org/10.3390/s20144031.

[25] T. Planès and E. Larose, "A review of ultrasonic Coda Wave Interferometry in concrete," *Cement Concr. Res.*, vol. 53, pp. 248–255, 2013, http://dx.doi.org/10.1016/j.cemconres.2013.07.009.

[26] A. Grêt, R. Snieder, and J. Scales, "Time-lapse monitoring of rock properties with coda wave interferometry," *J. Geophys. Res.*, vol. 111, pp. B03305, 2006, http://dx.doi.org/10.1029/2004JB003354.

[27] R. Snieder, A. Grêt, H. Douma, and J. Scales, "Coda Wave Interferometry for estimating nonlinear behavior in Seismic Velocity," *Science*, vol. 295, no. 5563, pp. 2253–2255, 2002, http://dx.doi.org/10.1126/science.1070015.

[28] A. Grêt, R. Snieder, and U. Ozbay, "Monitoring in situ stress changes in a mining environment with coda wave interferometry," *Geophys. J. Int.*, vol. 167, no. 2, pp. 504–508, 2006, http://dx.doi.org/10.1111/j.1365-246X.2006.03097.x.

[29] C. Hadziioannou, E. Larose, O. Coutant, P. Roux, and M. Campillo, "Stability of monitoring weak changes in multiply scattering media with ambient noise correlation: laboratory experiments," *J. Acoust. Soc. Am.*, vol. 125, no. 6, pp. 3688–3695, 2009, http://dx.doi.org/10.1121/1.3125345.

[30] C. Payan, V. Garnier, J. Moysan, and P. A. Johnson, "Determination of third order elastic constants in a complex solid applying coda wave interferometry," *Appl. Phys. Lett.*, vol. 94, no. 1, 2009, http://dx.doi.org/10.1063/1.3064129.

[31] F. D. Murnaghan, *Finite deformation of an elastic solid*, New York, NY, USA: John Wiley and Sons, Inc., 1951.

[32] E. Niederleithinger, P. Shokouhi, S. Stahler, and T. R. Nowak, “Detection of subtle changes in materials by coda wave interferometry”, in *Proc 10th European Conf. Non-Destructive Testing*, Moscow, June 7-11 2020, 2010.

[33] American Society for Testing and Materials, *Standard Specification for Portland Cement*, C150/C150M – 07, 2007.

[34] Associação Brasileira de Normas Técnicas, *Aggregates – Sieve analysis of fine and coarse aggregates*, NBR NM 248, 2003.

[35] P. K. Mehta and P. J. M. Monteiro, *Concrete: microstructure, properties and materials*, 3rd ed. New York, New York, USA: McGraw-Hill, 2006.

[36] P. A. Smith, "Stress-induced anisotropy in solids - the acousto-elastic effect," *Ultrasonics*, vol. 94, pp. 135–147, 1963.

[37] V. G. Haach, R. Carrazedo, P. O. Ribeiro, L. P. A. Ferreira, and I. P. Abe, "Evaluation of elastic anisotropic relations for plain concrete using ultrasound and impact acoustic tests," *J. Mater. Civ. Eng.*, vol. 33, pp. 1–14, 2020, http://dx.doi.org/10.1061/(ASCE)MT.1943-5533.0003562.

Author contributions: RMLG: methodology, formal analysis and investigation, writing. KFB: methodology, formal analysis and investigation, writing. VGH: conceptualization, methodology, formal analysis and investigation, writing, funding acquisition, resources, supervision.

Editors: Pedro Castro Borges, Guilherme Aris Parsekian.